BBC
BROWN BOVERI

PROTECTION OF LARGE INDUCTION MOTORS - PRACTICE VS. THE ACTUAL MODEL

STANLEY ZOCHOLL

BROWN BOVERI ELECTRIC
PROTECTIVE RELAY DIVISION
ALLENTOWN, PA.

EDMUND O. SCHWEITZER III

WASHINGTON STATE UNIVERISTY
PULLMAN, WASHINGTON

PRESENTED BEFORE THE ELEVENTH ANNUAL WESTERN PROTECTIVE RELAY CONFERENCE

OCTOBER 23, 24, 25, 1984
SPOKANE, WASHINGTON

PROTECTION OF LARGE INDUCTION MOTORS - PRACTICE VS. THE ACTUAL MODEL

ABSTRACT

This paper analyzes the relays used for thermal protection in induction motors. A computer simulation using thermal models of the motor is used to establish the correlation of the response of conventional relays with temperature rise in the motor. Although these relays respond only to current, it is shown that the temperature rise depends on specific thermal parameters, initial temperature and change in motor speed.

The paper discusses methods for determining the thermal parameters from motor data and the improvement in protection offered by microprocessor protective systems with algorithms based on the thermal models.

TABLE 1

STANDARD PROTECTIVE FUNCTIONS FOR INDUCTION MOTOR

ITEM	FUNCTION	PROTECTIVE RELAY	DEVICE	TRIP CRITERIA
1	Overload	Time-Overcurrent	51	OVER-TEMPERATURE
2	Overload & Locked Rotor	Time-Overcurrent	51	
3	Stator Temperature	Temperature	49T	
4	Unbalanced Current	Negative Sequence Overcurrent	46	
5	Short Circuit Protection	Instantaneous Overcurrent	50	OVERCURRENT
6	Ground Fault	Ground Sensor Residual Overcurrent Negative Sequence	50G 51N 46	
7	Differential	Self Balancing Percentage Differential	50 87	

INTRODUCTION

Table 1 shows the list of relays used to protect an induction motor in either the starting or the running state. They fall into two catagories.

Items 5, 6, and 7 are overcurrent, ground fault and differential relays which terminate short circuit current caused by faults in the machine. These relatively high speed devices are applied to limit damage and minimize the cost of repair.

The remaining relays are applied to prevent overheating in the machine caused by locked rotor, overload torque, high inertia starting or operation with unbalanced currents. With the exception of the 49T, these relays respond to current. Yet the trip criteria is really over-temperature in the stator or rotor. Whereas the conventional relays can only respond to current, it will be shown that temperature rise depends on initial temperature, specific thermal parameters, and in the rotor case, on slip as well.

In the paper, the correlation between relay travel and motor temperature rise is shown using a computer simulation. The simulation uses the state equations for the motor models given in reference (1) and the state equations for a conventional overcurrent relay. These are time discrete difference equations which describe the physical systems. These equations form the basis of a protective algorithm which a microprocessor can perform in real time. Consequently, the paper addresses the improvement in thermal protection achieved using a microprocessor based protective system and all pertinent parameters to determine conductor temperature.

The models used in the simulation are:

A. Positive and negative sequence electrical equivalent circuits of the motor used to determine stator and rotor current as a function of voltage and slip.

B. Thermal analog circuits for the stator and rotor used to determine temperature rise in the conductors as a function of watts in the electrical models.

C. Mechanical model using the summation of torque and the moment of inertia of motor and load acting on the shaft used to determine velocity acceleration and slip used in the electrical model.

The electrical and thermal models form the algorithm for the protective system.

ROTOR PROTECTION

Figures 1, 2, and 3 show the results of a study using a very inverse induction disk overcurrent relay for locked rotor protection of a large motor. Each diagram shows rotor current, temperature, torque, speed and relay travel versus time in seconds. Current is plotted in perunit of rated full load current with the relay set at two perunit current for pickup with maximum time dial. The displacement of the disk required for trip is 2π radians or 6.28 scale units and the temperature is scaled so this value corresponds to the predetermined trip temperature for the rotor.

Figure 1 shows the locked rotor case where the motor was energized with the rotor at zero degrees above ambient. This case shows good correlation between relay travel and temperature and the trip time is correct. However, the relay resets before the rotor can cool. Consequently, the motor overheats before the relay can trip if the motor is started at an elevated temperature as shown in Figure 2.

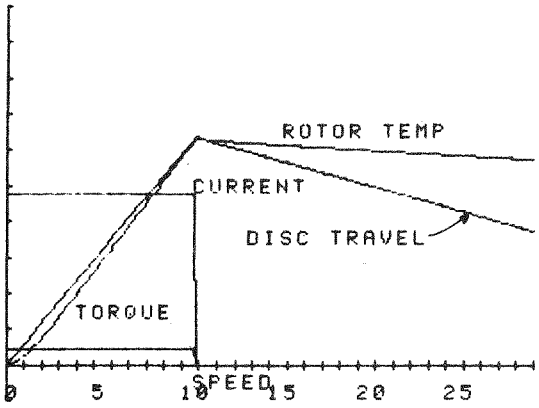

FIGURE 1. LOCKED ROTOR CASE SHOWING CORRELATION OF RELAY TRAVEL AND TEMPERATURE STARTING FROM AMBIENT.

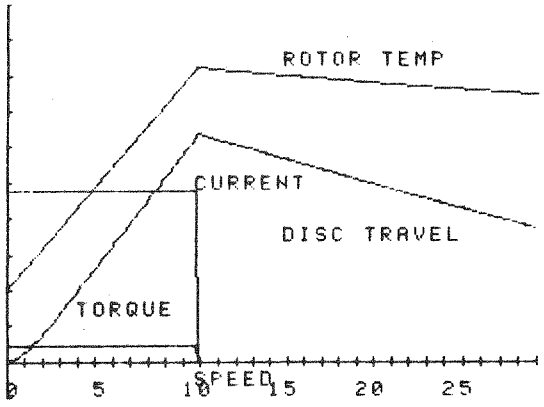

FIGURE 2. LOCKED ROTOR CASE SHOWING OVERHEATING CAUSED BY STARTING AT HIGH INITIAL TEMPERATURE.

Figure 3 shows a normal starting case where starting current brings the relay to the point of trip. The trip travel is almost identical to the locked rotor case because of the duration and magnitude of the starting current. However, the rotor temperature reaches only 70% of its critical temperature because the heat input to the rotor decreases with slip. Consequently, the relay travel does not correlate with temperature during a normal start and its over-response makes it difficult to use in the case of high inertia starting. It is seen that because the conventional overcurrent relay responds only to current it offers limited rotor protection.

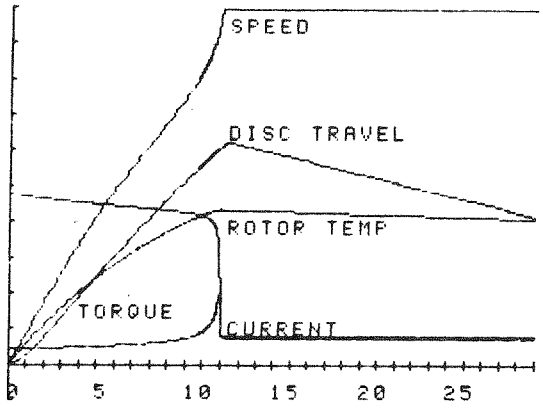

FIGURE 3. NORMAL START SHOWING DISC TRAVEL NEAR TRIP. TEMPERATURE AT 70%.

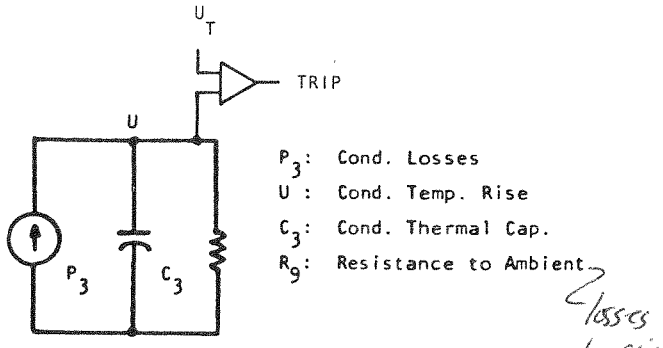

FIGURE 4. ROTOR THERMAL EQUIVALENT CIRCUIT

input = constant current input representing rotor losses

ROTOR THERMAL MODEL

The dynamic temperature rise in the rotor can be analyzed using the rotor thermal model shownin Figure 4. With properly identified parameters, it serves as the basis for the rotor protection algorithm. In the model the heat source P_3 is represented by a constant current numerically equal to the I^2R loss in the rotor. The voltage at the node U is the conductor temperature and the node capacitance C_3 represents the thermal capacitance of the rotor; conductor and core. Resistor Rq represents the thermal resistance accounting for the heat loss to ambient through the airgap and rotor shaft.

ROTOR HEAT SOURCE

Figures A1 and A2 in Appendix A present the traditional positive and negative sequence electrical models for the induction motor. The power delivered to the variable resistors in the two models represent the electromechanical power delivered by the motor. The power in the other resistors is dissipated as heat. These sources are the ones used at the inputs to the thermal models. The heat source for the rotor is given by:

$$P_3 = I_4^2 \ R_4 + I_5^2 \ R_5 \qquad (1)$$

where I_4 is the positive sequence rotor current

I_5 is the negative sequence rotor current

R_4 is the positive sequence rotor resistance (slip dep.)

R_5 is the negative sequence rotor resistance (slip dep.)

ROTOR RESISTANCE SLIP DEPENDENCE

The impedance of the rotor changes significantly with speed. This important phenomenon is caused by the slip frequency skin effect. When the rotor is still the positive sequence stator field travels at synchronous speed relative to the rotor. The voltage induced is at line frequency and the skin effect causes the majority of the current to flow at the outer edge of the conductor occupying only a third of the available cross-sectional area. The rotor resistance is high for this condition.

When the rotor accelerates, the speed relative to the rotor decreases and the frequency falls to only a fractional percent of the line frequency. The current then occupies the total area. The rotor resistance for this condition is low and the change from slip one to rated slip is of the order of 3 to 1.

This same phenomenon accounts for the increased heating of negative sequence current. Unbalanced current in the stator causes a negative sequence field which rotates in a direction opposite to that of the rotor. The voltage induced is double frequency and the majority of the negative sequence current in the rotor occupies only a sixth of the conductor. The negative sequence resistance is therefore still higher as is the heating effect. It is therefore important to represent the slip dependent rotor resistance in the thermal model.

Reference (2) shows that the change in rotor parameters are nearly linear with respect to slip as shown in Figure 5. Consequently, the resistance R_4 and R_5 are slip dependent and can be expressed as follows:

$$R_4 = (R_1 - R_0)\ S + R_0 \qquad (2)$$

$$R_5 = (R_1 - R_0)\ (2-S) + R_0$$

where R_1 = rotor resistance at S = 1

R_0 = rotor resistance at S = rated slip

R_1 and R_0 can be calculated from nameplate data using the torque relation $\tau=(I^2R_4)/S$. From this relation

$$R_4 = (\tau/I^2)\ S \qquad (3)$$

Where τ is torque, I is rotor current and S is slip. A sample calculation for a large induction motor is given in Appendix B. In this example, the ratio R_1/R_0 is 2.74 showing that the rotor heat decreases in this ratio as the motor accelerates.

SPEED ALGORITHM

It is not possible using conventional relaying to account for the varying value of slip. However, in the microprocessor system, slip can be obtained from voltage and current measured at the motor terminals. Using these values, the impedance looking into the machine is:

$$(V/I)= R + j\ X \qquad (4)$$

Reference (1) shows that slip can be calculated using the real part of this expression as follows:

$$S = R_0/(A(R-R_3) - (R_1 - R_0)) \qquad (5)$$

where R is the observed total resistance

R_3 is the stator resistance

R_0 is rated slip

R_1 is the locked rotor resistance

A is a factor relating rotor to stator current

In this equation R is the measurement and the remaining parameters are known constants which have been stored as part of the setting procedure.

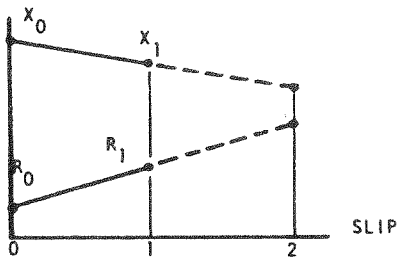

FIGURE 5. LINEAR APPROXIMATION OF SLIP DEPENDENT ROTOR RESISTANCE AND REACTANCE

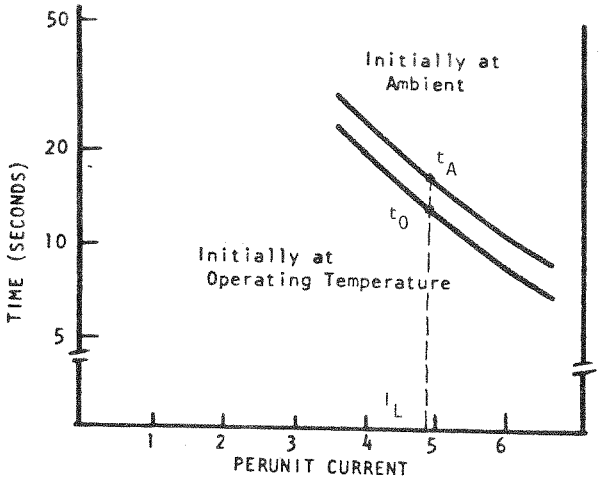

FIGURE 6. LOCKED ROTOR THERMAL LIMIT CURVE OBTAINED FROM MODEL

ROTOR THERMAL LIMIT CURVES AND PARAMETERS

The slip dependent heat source of the thermal model has been defined using nameplate data. The thermal parameters C_3 and R_9 can be scaled in terms of a locked rotor current I_L and two time values t_A and t_0 read from the thermal limit curves shown in Figure 6. These curves, issued by the motor manufacturer, take into account the rotor thermal capacitance. They define the time required for the locked rotor current to heat the rotor to a predetermined critical temperature. Two curves are required; one plotted with the motor initially at ambient and a second with the rotor initially at operating temperature.

Each point on the curve plotted from ambient represents the critical temperature. Each point also represents a constant I^2t value. Consequently, the value $I_L^2\ t_A$ corresponds to the critical temperature. For the locked rotor condition, the electrical resistance is R_1 and I^2R, equals the watts. In order to correlate directly with the curve, the heat source should be expressed in perunit I^2 rather than in perunit watts. This is done by dividing R_9 to express the heat in perunit of the load current heating effect. Consequently; the model parameters should be:

$$P_3 = I_1^2\ R_1/R_0$$

$$C_3 = R_1/R_0$$

$$U_{MAX} = I_L^2\ t\ A$$

Then for $I_1 = I_L$ and $U = I_L^2\ t_A$:

$$U = P_3\ t/C_3 = (I_L^2\ R_1/R_0)\ t\ /\ (R_1/R_0) = I_L^2\ t_A$$

$$t = t_A$$

as prescribed by the curve plotted with the rotor initially at ambient.

Since the points on both curves plotted in Figure 6 represent the same critical temperature, the $I^2 t$ difference in the curves represents the operating temperature. This is the steady state temperature caused by load current flowing in the thermal resistance. Therefore, $R_9 = I_L^2 (t_A - t_0)$, consequently a summary or rotor thermal parameters are as follows:

$$P_3 = I_L^2 (R_4/R_0) + I_2^2 (R_5/R_0)$$

$$C_3 = (R_1/R_0)$$

$$R_9 = I_L^2 (t_A - t_0)$$

$$U_T = x I_L^2 t_A$$

where x is a factor less than one so that the motor is tripped before the rotor critical temperature occurs.

STATOR PROTECTION

Rotor conductors are sized for high starting and the skin effect of the slip frequency may cause overheating during the starting period. However, during the running condition, the rotor current is uniformly distributed in the conductors and it is the stator winding that overheats during running overloads.

Standard overload protection includes both temperature and thermal overload relays. Temperature relays use bridge circuits to measure resistance temperature devices (RTD's) built into the insulation of the stator winding. The bridge voltage caused by a change in the RTD resistance is a direct measure of temperature of the insulation near the stator winding. Consequently, the relay can be set to either alarm at a predetermined critical temperature. Temperature relays provide excellent protection for creeping overloads where all parts of the motor heat uniformly. However, the RTD measures the insulation temperature and its response is too slow to detect the fast rise of conductor temperature caused by more severe or cyclic overloads. Therefore, thermal devices or long time overcurrent relays with slow reset are used to prevent stator overheating on severe overloads.

STATOR THERMAL MODEL

Conventional overload relays are poor models of the stator thermal circuit. Their response is that of a single-node thermal circuit with no attempt to match the stator thermal time constant. Consequently, their time-current characteristics are intended only to coordinate with the hot running overload curve of the motor with a conservative time margin. The stator must, therefore, be overprotected to compensate for the uncertainty of the thermal response.

An improvement can be made in the stator temperature estimate by first using a model where the thermal parameters match those of the stator. A still more accurate estimate is obtained when the RTD output is used as a feedback signal to update the temperature estimate. Once each sampling period, the microprocessor calculates the change in temperature and the RTD output. The difference between the RTD output and the estimate is used as an error signal to update the temperature estimate.

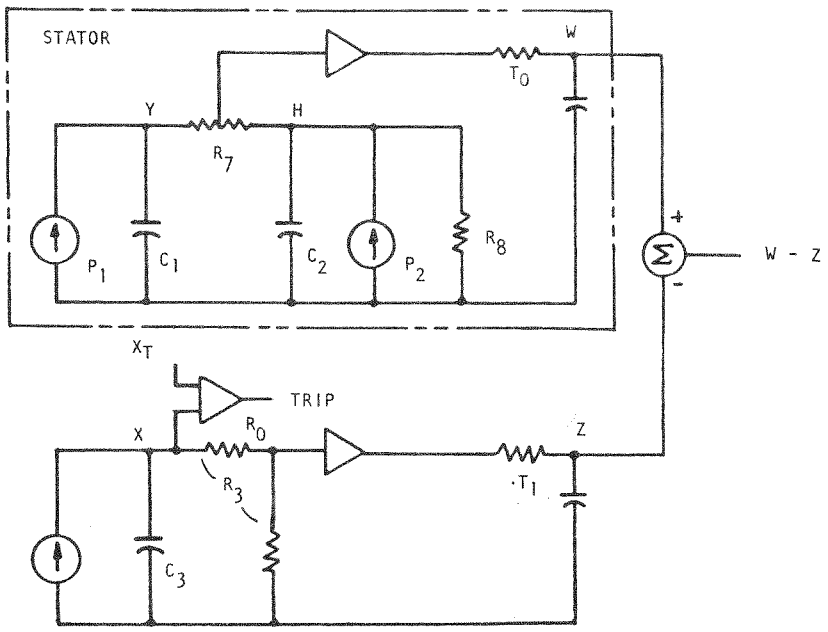

FIGURE 7. STATOR MODEL SHOWING RTD FEEDBACK

This technique can be analyzed using the models shown in Figure 7. The more complex thermal model represents the actual stator. The RTD is shown as a buffered RC circuit with time constant T_0. Its location is represented by a point in the thermal resistance R_7 which accounts for the heat conducted from the conductors to the iron core through the winding insulation.

In this model Y is the conductor temperature and H is the temperature of the iron core. C_1 and C_2 are the thermal capacitances of the conductor and the iron and R_8 accounts for the heat conducted from the iron to the ambient. The conductors are heated by the conductor loss P_1 and the iron by the core loss watts P_2.

The more simple model called the filter is the one used in the protection algorithm to obtain the estimate of the conductor temperature X and the RTD output Z. In this model P_1 and C_3 correspond to P_1 and C_1 of the stator. R_3 equals the total thermal resistance R_7 and R_8 of the stator and the time constant T_1 should equal T_0 of the stator model. The position of the RTD in the filter model is determined by the resistance value R_0.

The procedure for obtaining the corrected temperature estimates using the filter is as follows. The time discrete state equation for the filter using a time step of T is:

$$\begin{bmatrix} X \\ Z \end{bmatrix} = \begin{bmatrix} (1 - T/R_3\ C_3) & 0 \\ (TR_0/R_3\ T_1) & (1-T/T_1) \end{bmatrix} \begin{bmatrix} X_0 \\ Z_0 \end{bmatrix} + \begin{bmatrix} T/C_3 \\ 0 \end{bmatrix} P_1$$

The equation determines a new set of values (X, Z) from present values (X_0, Z_0) and the input P_1. The new values are corrected as follows:

$$X_0 = X = K_1 \ (W - Z)$$

$$Z_0 = Z + K_2 \ (W - Z)$$

where K_1 and K_2 are the Kalman gains for the filter and are predetermined from stator thermal parameters. Specifically, the thermal time constants R_3 C_3 and T, determine K_1 and K_2.

Values for R_3 and C_3 can be derived from stator I^2t thermal limit curves using the method described above. The RTD tap resistance R_0 by the assumption that the RTD reads 10 degrees less than the rated conductor temperature. Consequently; $R_0 = (T_R - 10^o) R_3/T_R$ where T_R is rated temperature rise for the stator winding.

The effect of the Kalman gains are shown by the results of the overload study plotted in Figures 8 or 9. In this study a cyclic 1.4 perunit overload is applied for ten minutes and then removed for five. The thermal time constant for the motor is 250 seconds with an RTD time constant of 20 seconds.

In Figure 8, the Kalman gains are set to zero and the filter estimates X and Z cannot track the more complex response of the stator temperature Y and RTD output W. The error (X-Y) is plotted to show its magnitude relative to the stator temperature Y.

Figure 9 shows the same study with Kalman gains K_1 and K_2 set to 0.26 and 1.0. The corrected estimates X and Z now match the actual values Y and W.

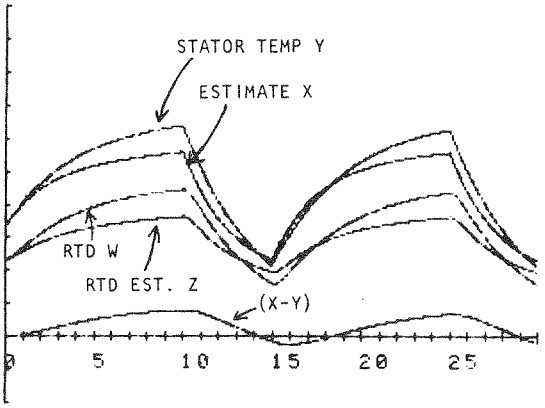

FIGURE 8. STATOR AND RTD TEMPERATURE COMPARED TO FILTER ESTIMATED VALUES WITH $K_1 = K_2 = 0$

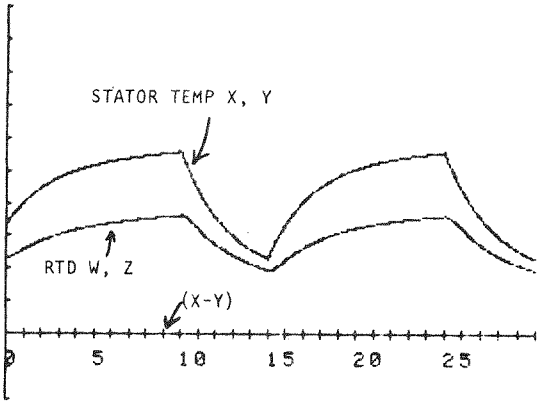

FIGURE 9. STATOR AND RTD TEMPERATURE COMPARED TO ESTIMATED VALUES $K_1 = .26$, $K_2 = 1.0$

CONCLUSIONS:

1. Adequate thermal protection of induction motors can be provided by conventional overcurrent and thermal relays under restricted operating conditions. These relays respond only to current and cannot emulate specific thermal parameters or initial conditions.

2. Accurate estimates of rotor and stator temperature are obtained from electrical and thermal models of the induction motor incorporating a speed algorithm.

3. Such models identify parameters required for motor protection which can be derived from nameplate data and thermal limit curves.

4. The models are ideal elements for motor protection since they respond directly to temperature. Settings of temperature thresholds and parameters secure thermal protection under difficult conditions of unbalance, overload, and high inertia starting.

APPENDIX A - INDUCTION MOTOR

ELECTRICAL MODELS

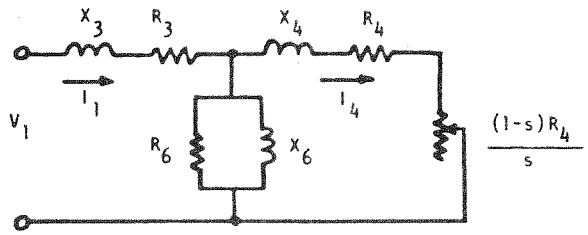

FIGURE A1. POSITIVE SEQUENCE ELECTRICAL MODEL

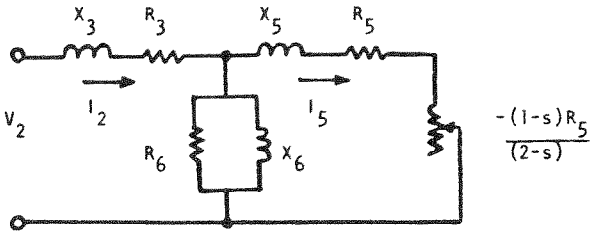

FIGURE A2. NEGATIVE SEQUENCE ELECTRICAL MODEL

Figures A1 and A2 present traditional electrical models for the positive and negative sequences. The circuit elements are defined as follows:

V_1	Positive-sequence terminal voltage
I_1	Positive-sequence input current
I_4	Positive-sequence rotor current
V_2	Negative-sequence terminal voltage
I_2	Negative-sequence input current
I_5	Negative-sequence rotor current
R_3+jX_3	Stator impedance
R_4+jX_4	Positive-sequence rotor impedance (slip dep.)
R_5+jX_5	Negative-sequence rotor impedance (slip dep.)
S	Per-unit slip
X_6	Magnetizing reactance
R_6	Non-linear resistance representing core losses

APPENDIX B - CALCULATION OF R_1 and R_0

The locked rotor resistance R_1 and the running resistance R_0 define the slip dependency of the rotor resistance. They can be defined from nameplate data

using the torque relation $\tau = I_1^2 R_4 / S$; consequently,

$$R_4 = (\tau/I^2) S$$

where R_4 = perunit rotor resistance

τ = torque in perunit of full load torque

I = Rotor current in perunit of full load

S = Slip

Values for R_1 and R_0 can be derived from the following typical motor data:

Speed: 1800 RPM synchronous
1787 RPM full load

Current: 667 amps full load
3941 amps locked

Torque: 52,894 lb. ft. full load
36,606 lb. ft. locked

Running Resistance R_0 $\quad I = 1, \tau = 1$

$$R_0 = S_0 = (1800-1787)/1800 = .0072$$

Locked Rotor Resistance R_1

$$T_L = 36,606/52,894 = .692 \text{ P.U.}$$

$$I_L = 3941/667 = 5.91 \text{ P.U.}$$

$$R_1 = (.694/5.91)^2 \times 1 = .0198$$

REFERENCES

1. Zocholl, S.E., Schweitzer III, E.O., Aliaga-Zegarra, A., "Thermal Protection of Induction Motors Enhanced by Interactive Electrical and Thermal Models". IEEE Transactions, Vol. PAS-103, No. 7, July 1984, pp 1749-1756

2. Gafford, B.N., Duesterheoft Jr., W.C., Mosher III, C.C., "Heating of Induction Motors on Unbalanced Voltages." AIEE Transaction, June 1959, pp 282-287.

3. Martiny, W.J., McCoy, R.M., Margolis, H.B., "Thermal Relationships in an Induction Motor Under Normal and Abnormal Operation." AIEE Transactions PAS, Presented at AIEE Winter General Meeting, New York, NY, January 31-February 5, 1960.

4. Cummings, P.G., Bowers, W.D., Martiny, W.J. "Induction Motor Efficiency Test Methods." IEEE Transactions on Industry Applications. Vol. IA-17 No. 3, May/June 1981, pp 253-272.

5. IEEE Trial-Use Guide for Construction and Interpretation of Thermal Limit Curves for Squirrel-Cage Motors over 500 HP, ANSI/IEEE Std. 620, April, 1981.

6. Eliasen, A.N. "The Protection of High-Inertia Drive Motors During Abnormal Starting Conditions." IEEE Transactions, Vol. PAS-99, No. 4, July/August 1980.

7. Eliasen, A.N. "High-Inertia Drive Motors and Their Starting Characteristics." IEEE Transactions, Vol. PAS, No. 4, July/August 1980, pp 1472-1482.